

## Performance of carbon nanotube-dispersed thin-film transistors

S. Kumar<sup>a)</sup>

Network for Computational Nanotechnology, Purdue University, West Lafayette, Indiana 47906

G. B. Blanchet

Dupont Central Research, Wilmington, Delaware 19880

M. S. Hybertsen

Center for Electron Transport in Molecular Nanostructures, Columbia University, New York, New York 10027

J. Y. Murthy and M. A. Alam

Network for Computational Nanotechnology, Purdue University, West Lafayette, Indiana 47906

(Received 7 June 2006; accepted 9 August 2006; published online 2 October 2006)

A numerical technique that relies on modifying the organic semiconducting host with metallic carbon nanotubes (CNTs) to increase the transconductance or, equivalently, reduce effective channel length ( $L_{\text{eff}}$ ) has recently been proposed. The authors use an extensive set of experimental data to analyze the performance of these transistors using the theory of heterogeneous two-dimensional percolating networks of metal-semiconducting CNTs embedded in the organic host. Their analysis (i) reproduces experimental characteristics, (ii) shows that  $L_{\text{eff}}$  scales as a power law of CNT-doping density ( $\rho$ ), (iii) illustrates the importance of an active subpercolating network of semiconducting CNTs in an organic host, and (iv) establishes the upper limit of transistor count for an integrated circuit based on this technology as a function of  $\rho$ , on current ( $I_{\text{on}}$ ), and circuit-failure probability ( $F$ ). © 2006 American Institute of Physics. [DOI: 10.1063/1.2357852]

Organic thin-film transistors (TFTs) have been the subject of intense research for possible applications in electronics displays, sensors, rf-ID tags, etc.<sup>1-6</sup> If the transconductance ( $g_m$ ) of organic TFTs could be further improved, the technology could potentially compete for applications currently based on more-expensive amorphous-Si or poly-Si TFTs.  $g_m$  can be improved either by enhancing mobility ( $\mu$ ) (which is limited by extrinsic effects<sup>1</sup>) or by decreasing the channel length ( $L_C$ ) (dictated by lithography). An approach involving modifying the transconductance of an organic host with carbon nanotubes (CNTs) has recently been proposed. A 60-fold decrease in  $L_C$  is observed that results in a similar increase in  $g_m$  with a negligible change in on-off ratio.<sup>1</sup> In this technique, the majority of the current paths are formed by the network of CNTs, but short switchable semiconducting links are required to complete the channel path from source to drain,<sup>1</sup> effectively reducing the lithography-limited  $L_C$  to the electrically relevant,  $L_{\text{eff}}$ . One of the important advantages of this technique is that it provides an inexpensive printing capability to get effectively lower  $L_C$  (high  $g_m$ ) without requiring expensive, high resolution lithographic techniques required for state-of-the-art silicon microelectronics.<sup>1</sup> The transport properties of this CNT-organic matrix composite are controlled by the statistical properties of the embedded heterogeneous CNT network and its interaction with the organic matrix. A rigorous physics-based model is required to interpret experimental results and predict trends, accounting for the interfacial properties of the dispersion and host materials.

In this letter, we present the effect of CNT dispersion in a semiconducting host on the improved performance of organic transistors in terms of the effective channel length

( $L_{\text{eff}}$ ) for different network densities ( $\rho$ ). We represent the organic-CNT network transistor [see Fig. 1(a)] as a two-dimensional percolating random network of nanotubes of length  $L_t$  and diameter  $d$  dispersed in an organic matrix of (geometrical) channel length  $L_C$  and channel width  $H$ . We

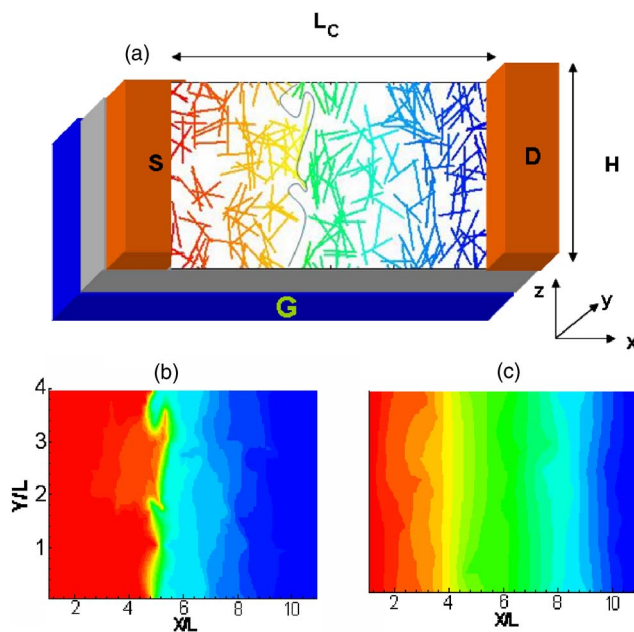


FIG. 1. (Color online) (a) Organic thin-film network transistor with channel length  $L_C$ , channel width  $H$ , and individual tube length  $L_t$ . Source ( $S$ ), drain ( $D$ ), and gate ( $G$ ) are also indicated. The clusters of nanotubes on the left and right sides of the black curve are not connected. The potential distribution in the CNT network is also shown. (b)  $X$ - $Y$  cross section through the organic substrate of the TFT in (a) showing contours of potential distribution.  $L_t=1 \mu\text{m}$ ,  $L_C=10 \mu\text{m}$ ,  $H=4 \mu\text{m}$ , and  $\rho=5 \mu\text{m}^{-2}$ . (c)  $X$ - $Y$  cross section through the organic substrate of the TFT showing contours of potential distribution.  $L_t=1 \mu\text{m}$ ,  $L_C=10 \mu\text{m}$ ,  $H=4 \mu\text{m}$ , and  $\rho=1 \mu\text{m}^{-2}$ .

<sup>a)</sup>Electronic mail: kumar21@purdue.edu

validate the  $\rho$ - $L_{\text{eff}}$  dependence by experiments and numerical simulations. The computational model is also used to illustrate the surprising role of semiconducting tubes in interpreting some of the previously unexplained experimental features.<sup>1</sup> Finally, we calculate the fluctuations in transistor performance as well as the probability of electrical short circuit due to fluctuation in  $L_{\text{eff}}$  as a function of  $\rho$ . Given an acceptable yield (e.g., 90%–99%) and minimum drive current  $I_{\text{on}}$ , our analysis establishes the upper limit of the number of transistor in an integrated circuit ( $N_{\text{max}}$ ) as a function of CNT density  $\rho$ .

For the organic transistors under consideration, since  $L_C \gg \lambda$ , the mean free path for electrons, we may use semiclassical transport theory (drift-diffusion theory based on Kirchoff's law for the linear regime) to analyze device characteristics.<sup>7–11</sup> The current along the tube is given by  $J = q\mu n(V_{GS})d\phi(V_{DS})/ds$ . Using the current continuity equation  $dJ/ds = 0$  and accounting for charge transfer to intersecting tubes as well as to the substrate, the dimensionless potential distribution  $\phi_i$  along tube  $i$  as well as the three-dimensional potential field in the substrate are given by

$$\frac{d^2\phi_i}{ds^2} + \sum_{\text{intersecting tubes } j} c_{ij}(\phi_j - \phi_i) + d_{is}(\phi_s - \phi_i) = 0, \quad (1a)$$

$$\nabla^2\phi_s + \sum_{i=1}^{N_{\text{tubes}}} d_{is}\beta_v \frac{\sigma_i}{\sigma_s}(\phi_i - \phi_s) = 0. \quad (1b)$$

Here  $s$  is the length along the tube (normalized to grid spacing) and  $c_{ij} = G_0/G_1$ , where  $G_0$  and  $G_1$  are the mutual and self-conductance of the tubes, respectively.<sup>7</sup> The quantity  $c_{ij}$  is the dimensionless charge-transfer coefficient between tubes  $i$  and  $j$  at their intersection point and is specified *a priori*; it is nonzero only at the point of intersection. The term  $d_{is}$  represents the dimensionless charge-transfer coefficient between the tube and substrate. The tube to substrate electrical conductivity ratio is  $\sigma_i/\sigma_s$ . The geometric parameter  $\beta_v$  and applied boundary conditions are explained in Ref. 12. The problem is solved numerically using the finite volume method.<sup>7,13</sup> This computation of voltage distribution is only valid for linear regime ( $\sim$  low  $V_{DS}$ ). The results from the simulation are discussed below.

To illustrate the basic technique, we compute the voltage distribution inside the organic matrix and the CNT network for  $L_C = 10 \mu\text{m}$ ,  $L_t = 1 \mu\text{m}$ ,  $H = 4 \mu\text{m}$ ,  $V_{DS} = -10 \text{V}$ , and  $V_{GS} = -100 \text{V}$ .<sup>1</sup> Voltage contour plots are shown in Fig. 1 to visualize the CNT-organic interaction. As a first illustration, we only disperse metallic CNTs with  $\rho = 5.0 \mu\text{m}^{-2} < \rho_{\text{th}}$  for metallic percolation.<sup>14</sup> The interconnected cluster of metallic CNTs at the left and right of the black curve (drawn manually to show disconnection in CNT clusters) in Fig. 1(a) is electrically isolated such that the charge can flow from the left island to the right only through the switchable stretches of semiconducting organic matrix (hypothesis proposed in Ref. 1). As a result, there is large voltage drop in the low-mobility organic matrix around this region, as shown in Fig. 1(b). This interpretation of “statistical shortening” of the channel by CNT doping of the organic host ( $L_{\text{eff}}$  depends on the sample because the geometry of metallic clusters is sample specific) is consistent with the hypothesis proposed in Ref. 1. For low network densities ( $\rho = 1.0 \mu\text{m}^{-2}$ ), the volt-

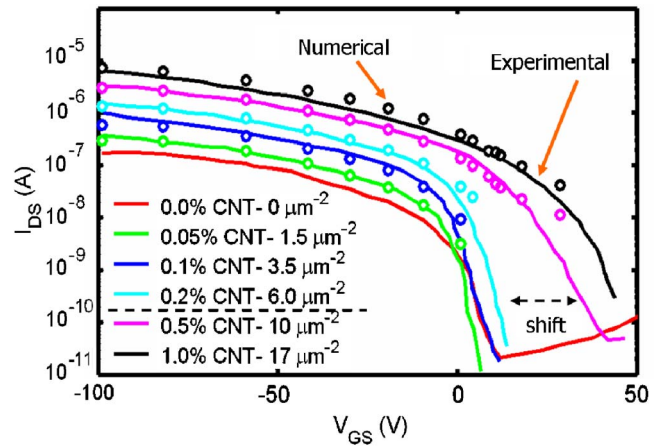


FIG. 2. (Color online) Computed  $I_{DS}$ - $V_{GS}$  at  $V_{DS} = -10 \text{V}$  for different CNT densities ( $\rho \sim 1$ – $17 \mu\text{m}^{-2}$ ) is compared with experimental results in Ref. 1. The vol % of CNT dispersions used in the experiments and the corresponding network density ( $\rho \sim \mu\text{m}^{-2}$ ) used in the computations are shown.  $L_t = 1 \mu\text{m}$ ,  $L_C = 20 \mu\text{m}$ , and  $H = 200 \mu\text{m}$ . The shift in the  $I_{DS}$ - $V_{GS}$  curves due to the start of semiconducting-CNT percolation for CNT vol %  $> 0.2\%$  is shown by the dashed line.

age contours in the substrate are much less distorted and the voltage varies approximately linearly from source to drain, Fig. 1(c).

Although our initial numerical model with *only* metallic-CNT dispersions validates the general assertion in Ref. 1, there is an anomalous jump in the  $I_{DS}$ - $V_{GS}$  curve along the  $V_{GS}$  axis for 0.5% volume fraction of CNTs [see Fig. 1(b), Ref. 1] which is not properly understood within this framework. We now calculate the  $I_{DS}$ - $V_{GS}$  characteristics of the organic TFT device in Ref. 1 with a realistic heterogeneous network of semiconducting-metallic tubes (1:2 ratio) dispersed in an organic matrix to show that this anomalous shift in  $I_{DS}$ - $V_{GS}$  curve is a consequence of the formation of a parallel subpercolating network of *semiconducting* CNTs inside the organic matrix.

The device parameters  $L_C = 20 \mu\text{m}$ ,  $L_t = 1 \mu\text{m}$ , and  $V_{DS} = -10 \text{V}$  are chosen to match the experiments in Ref. 1. We checked the sensitivity of our results to various probability distributions of tube lengths confined to 0.5– $1.5 \mu\text{m}$ . We find less than 10% variation in  $I_{DS}$ , which is well within the experimental-error margin. Charge-transfer coefficients  $c_{ij} = 10^{-4}$  and  $d_{is} = 10^{-4}$  are assumed and correspond to poor contact conductance between tube-tube and tube-substrate. The electrical conductivity ratio,  $\sigma_i/\sigma_s$ , for metallic CNTs in the on state ( $V_{GS} = -100 \text{V}$ ) is taken as  $5.0 \times 10^4$ , while that for semiconducting CNTs is  $5.0 \times 10^3$ .<sup>15</sup> The metallic-CNT conductivity is assumed constant with  $V_{GS}$ , while the rolloff in the conductivity of semiconducting CNTs and the organic matrix with  $V_{GS}$  is obtained from the experimental  $I_{DS}$ - $V_{GS}$  curves (0% and 0.5% volume fraction curves) in Fig. 1(b) of Ref. 1. Figure 2 shows that numerical results agree well with experiments over the entire range of tube densities ( $1.5$ – $17 \mu\text{m}^{-2}$ ). The anomalous shifts of  $I_{DS}$ - $V_{GS}$  curves are also properly captured by our numerical simulations, Fig. 2; this confirms that semiconducting CNTs are active elements of this organic TFT device.

Since the performance of the organic transistor depends on  $g_m$  ( $\sim 1/L_{\text{eff}}$ ), optimization and circuit design with these CNT-doped organic-TFTs require explicit specification of  $L_{\text{eff}}$  as a function of  $\rho$ . We disperse CNTs in different volume

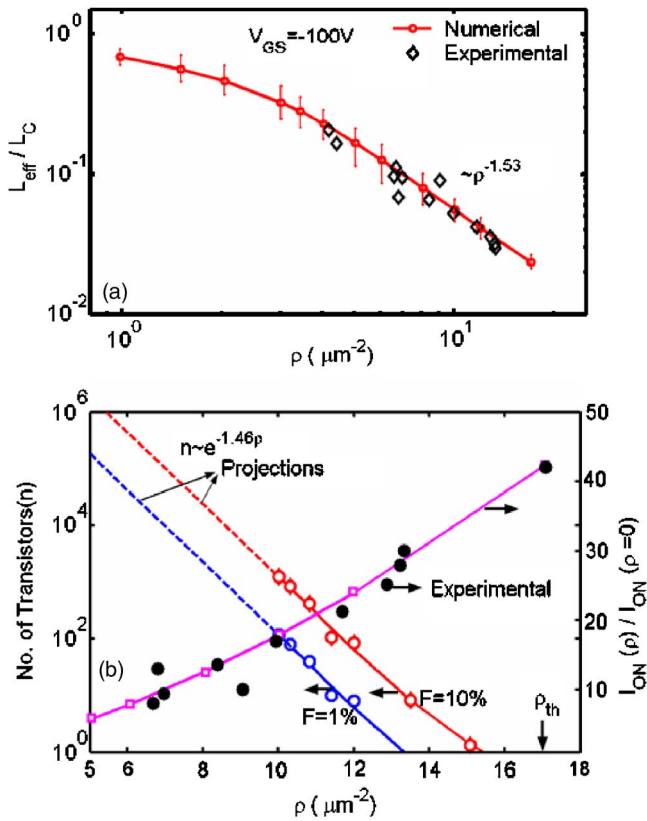


FIG. 3. (Color online) (a) Effective reduction in channel length ( $L_{\text{eff}}$ ) against density ( $\rho$ ) for gate voltage  $V_{GS} = -100\text{ V}$ . The power-law exponents ( $m$ ) for high-density CNT dispersions are also shown. The error bars reflect the statistical measure of the variation across the ensemble.  $L_t = 1\ \mu\text{m}$ ,  $L_C = 20\ \mu\text{m}$ , and  $H = 200\ \mu\text{m}$ . (b) Number of transistors in the circuit against  $\rho$  for  $F = 1\%$  and  $10\%$  (left side). Normalized on current of the transistor against  $\rho$  (right side).  $V_{GS} = -100\text{ V}$ ,  $L_t = 1\ \mu\text{m}$ ,  $L_C = 20\ \mu\text{m}$ , and  $H = 200\ \mu\text{m}$ . For  $\rho < 10\ \mu\text{m}^{-2}$ , the projections for  $n$  are shown by dashed lines.

fractions in polythiophene organics and measured  $I_{\text{on}}$  (for fabrication details, see Ref. 1). The density of the CNT network ( $\rho$ ) is measured using atomic force microscopy. Figure 3(a) shows that for reasonably high densities ( $\rho > 3\ \mu\text{m}^{-2}$ ), a power-law dependence of  $L_{\text{eff}}$  on  $\rho$  is observed with a power exponent of 1.53, i.e.,  $L_{\text{eff}} \sim \rho^{-1.53}$ . Our numerical simulations with similar device parameters ( $L_C = 20\ \mu\text{m}$ ,  $L_t = 1\ \mu\text{m}$ , and  $V_{DS} = -10\text{ V}$ ) and based on the average of 200 samples show similar power-law behavior and have excellent agreement with the experimental power exponent ( $< 1\%$  variation), Fig. 3(a).

To use these organic transistors as circuit elements for large-area applications, it is important to analyze the fluctuation of transistor performance (across an ensemble of CNT-dispersed organic transistors nominally at the same average concentration) to determine the probability of an electrical short-circuit (by metallic tubes) as a function of CNT density. We analyze the statistical fluctuation by computing  $L_{\text{eff}}/L_C$  over 200 different random ensembles of the CNT-organic transistor for different  $\rho$  ( $1 - 17\ \mu\text{m}^{-2}$ ), Fig. 3(a). As a general rule, normalized  $I_{\text{on}}$  increases and normalized fluctuation ( $\Delta L_{\text{eff}}$ ) decreases with higher  $\rho$ , both desirable features for high performance ICs. However, a calculation of the percentage of failed transistors  $f$  (by determining ratio of transistors above the metallic-percolative threshold based on an ensemble of 4000 random samples) shows that circuit-

failure probability  $F$ , given by  $1 - F = (1 - f)^n$ , also increases dramatically at higher densities ( $F$  is fixed by yield target,  $f$  is simulated to infer  $n$ ). This opposing trend of transistor count  $n$  ( $n \sim e^{-1.46\rho}$  for  $\rho < 12\ \mu\text{m}^{-2}$ ) and drive current  $I_{\text{on}}$  [see Fig. 3(b)] with respect to  $\rho$  defines the essence of the optimization issue for CNT-doped organic transistors.

In summary, a computational diffusive-transport model is developed to explore the performance of organic transistors with a randomly dispersed CNT network. A power-law behavior for  $L_{\text{eff}}$  against  $\rho$  is observed both from the numerical model and experimental measurements. Computational analysis establishes the importance of active subpercolating networks of semiconducting CNTs. The present framework for analyzing optimum  $\rho$  based on  $I_{\text{on}}$ ,  $F$ , and performance fluctuation is useful in the analysis, optimization, and development of future organic electronics. Furthermore, the model can easily be extended to predict the thermal, magnetic, and other macroscopic transport properties of CNT-matrix mixtures<sup>16,17</sup> or other long-aspect ratio suspensions (DNA) used in a wide range of applications.<sup>18,19</sup>

<sup>1</sup>X. Z. Bo, C. Y. Lee, M. S. Strano, M. Goldfinger, C. Nuckolls, and G. B. Blanchet, Appl. Phys. Lett. **86**, 182102 (2005).

<sup>2</sup>C. Dimitrakopoulos and D. Mascaró, IBM J. Res. Dev. **45**, 11 (2001).

<sup>3</sup>H. Siringhaus, T. Kawase, R. H. Friend, T. Shimoda, M. Inbasekaran, W. Wu, and E. P. Woo, Science **290**, 2123 (2000).

<sup>4</sup>G. B. Blanchet, Y. L. Loo, J. A. Rogers, C. R. Fincher, and F. Gao, Appl. Phys. Lett. **82**, 463 (2003).

<sup>5</sup>J. A. Rogers, Z. Bao, K. Baldwin, A. Dodabalapur, B. Crone, V. R. Raju, V. Kuck, H. Katz, K. Amundson, J. Ewing, and P. Drzaic, Proc. Natl. Acad. Sci. U.S.A. **98**, 4835 (2001).

<sup>6</sup>C. J. Drury, C. M. J. Mutsaers, C. M. Hart, M. Hatters, and D. M. Leeuw, Appl. Phys. Lett. **73**, 108 (1998).

<sup>7</sup>S. Kumar, J. Y. Murthy, and M. A. Alam, Phys. Rev. Lett. **95**, 066802 (2005).

<sup>8</sup>S. Datta, *Quantum Transport: Atom to Transistor*, 2nd ed. (Cambridge University Press, Cambridge, 2005), Vol. 1, pp. 104-154.

<sup>9</sup>M. S. Fuhrer, J. Nygrd, L. Shih, M. Forero, Y. G. Yoon, M. S. C. Mazzoni, H. J. Choi, J. Ihm, S. G. Louie, A. Zettl, and P. L. McEuen, Science **288**, 494 (2000).

<sup>10</sup>R. F. Pierret, *Semiconductor Device Fundamentals* (Addison-Wesley, New York, 1996), Vol. 1, pp. 75-138.

<sup>11</sup>S. Kumar, N. Pimparkar, J. Y. Murthy, and M. A. Alam, Appl. Phys. Lett. **88**, 123505 (2006).

<sup>12</sup>The geometric parameter  $\beta_0$  is given by  $\beta_0 = \alpha_v A_t / P_s$ , where  $\alpha_v$  is the contact area of the tube per unit volume of the substrate,  $A_t$  is tube cross-section area, and  $P_s$  is the tube perimeter. For computing voltage distribution, boundary conditions  $\phi_t = 1.0$  and  $\phi_t = 0$  are applied to the tube tips embedded in the source and drain regions, respectively. Similarly, for the organic substrate,  $\phi_s = 1.0$  and  $\phi_s = 0$  are applied at the source and drain ends, respectively. The boundaries,  $y^* = 0$  and  $y^* = H/d$ , are assumed as periodic boundaries for both substrate and tubes.

<sup>13</sup>S. V. Patankar, *Numerical Heat Transfer and Fluid Flow* (Hemisphere, New York, 1980), Vol. 1, pp. 25-39.

<sup>14</sup>It has been reported in Ref. 1 that transistors get shorted at 1% volume fraction of CNT or greater, implying that metallic CNTs begin to percolate at this volume fraction. From Ref. 11, the percolation threshold for the CNT network is given by  $\rho_{\text{th}} = 4.236^2 / \pi L_t^2 = 5.7\ \mu\text{m}^{-2}$  using an average tube length of  $1\ \mu\text{m}$  (Ref. 1). Accounting for the fact that one-third of the CNTs are metallic, the total density  $\rho$  of the CNTs at 1% volume fraction may be computed as  $\rho = 3 \times 5.7 = 17.1\ \mu\text{m}^{-2}$ . Using this conversion, the volume fraction data in Ref. 1 may be converted into the area density  $\rho$  needed for our computation.

<sup>15</sup>R. V. Seidel, A. P. Graham, B. Rajasekharan, E. Unger, M. Liebau, G. S. Duesberg, F. Kreupl, and W. J. Hoenlein, J. Appl. Phys. **96**, 6694 (2004).

<sup>16</sup>C. W. Nan, G. Liu, Y. Lin, and M. Li, Appl. Phys. Lett. **85**, 3549 (2004).

<sup>17</sup>A. N. Lagarkov and A. K. Sarychev, Phys. Rev. B **53**, 6318 (1996).

<sup>18</sup>O. G. Berg, R. B. Winter, and P. H. Hippel, Biochemistry **20**, 6929 (1981).

<sup>19</sup>K. V. Klenin, H. Merlitz, J. Langowski, and C. X. Wu, Phys. Rev. Lett. **96**, 018104 (2006).